Discussion des résultats

Les distances et angles obtenus par Takenaka *et al.* (1970) sont souvent voisins des nôtres (Tableaux 3 et 4), mais donnés avec des déviations standard 4 fois plus grandes. Toutefois dans le cycle pyridinique de Takenaka *et al.* (1970) les deux distances C–N sont assez différentes 1,351 (12) et 1,312 (12) au lieu de 1,337 (2) et 1,340 (2) pour ce travail. Pour l'entourage de l'atome de cuivre, Takenaka *et al.* donnent 1,935 (9) Å pour la liaison Cu–O et 1,974 (12) Å pour la liaison Cu–N alors que nous avons respectivement obtenu 1,940 (2) et 1,963 (2) Å, valeurs d'autre part très voisines de celles obtenues par Stephens (1970) pour le composé d'addition: picolate de cuivre, thiocyanate de potassium $Cu(C_5H_4N\text{-}COO)_2.KSCN$: Cu–O = 1,942 (5) et Cu–N = 1,961 (6) Å.

Tableau 3. *Distances interatomiques*

		Takenaka *et al.*
Cu—N	1,963 (2) Å	1,974 (12) Å
N—C(1)	1,337 (2)	1,312 (12)
C(1)–C(2)	1,382 (2)	1,383 (13)
C(2)–C(3)	1,388 (3)	1,378 (14)
C(3)–C(4)	1,377 (4)	1,374 (16)
C(4)–C(5)	1,381 (3)	1,369 (14)
C(5)–N	1,340 (2)	1,351 (12)
C(1)–C(6)	1,508 (3)	1,519 (13)
C(6)–O(1)	1,234 (2)	1,222 (12)
C(6)–O(2)	1,276 (2)	1,297 (11)
O(2)–Cu	1,940 (2)	1,935 (9)
Cu—O(1^{ii})	2,752 (2)	2,754 (11)

Tableau 4. *Angles*

		Takenaka *et al.*
Cu—N—C(1)	112,1 (1)°	112,1 (5)°
N—C(1)–C(2)	122,1 (2)	122,1 (8)
N—C(1)–C(6)	114,1 (1)	115,2 (8)
C(6)–C(1)–C(2)	123,7 (2)	122,7 (8)
C(1)–C(2)–C(3)	118,0 (2)	117,6 (9)
C(2)–C(3)–C(4)	119,6 (2)	120,5 (10)
C(3)–C(4)–C(5)	119,4 (2)	118,7 (10)
C(4)–C(5)–N	121,0 (2)	120,8 (10)
C(5)–N—C(1)	119,9 (2)	120,4 (9)
C(5)–N—Cu	127,9 (2)	127,3 (5)
C(1)–C(6)–O(1)	119,9 (2)	121,4 (7)
C(1)–C(6)–O(2)	115,1 (1)	113,4 (7)
O(1)–C(6)–O(2)	125,0 (2)	125,2 (8)
C(6)–O(2)–Cu	114,5 (1)	115,0 (5)
O(2)–Cu—N	83,6 (1)	83,5 (3)

Références

D'Ascenzo, G. & Wendlandt, W. W. (1970). *Anal. Chim. Acta*, **50**(1), 79–91.

Faure, R. (1973). Thèse, Lyon.

Faure, R. & Loiseleur, H. (1972). *Acta Cryst.* B**28**, 2733–2740.

Gillard, R. D., Laurie, S. H. & Stephens, F. S. (1968). *J. Chem. Soc.* (*A*), pp. 2588–2589.

Kleinstein, A. & Webb, G. A. (1971). *J. Inorg. Nucl. Chem.* **33**, 405–412.

Stephens, F. S. (1970). *J. Chem. Soc.* (*A*), pp. 2377–2379.

Takenaka, A., Utsumi, H., Yamamoto, T. & Furusaki, A. & Nitta, I. (1970). *Nippon Kagaku Zasshi*, **91**(10), 928–935.

Thomas, G. (1960). Thèse, Lyon.

Acta Cryst. (1973). B**29**, 1893

X-ray Diffraction Determination of the Crystal Structure of 1,3,5-Triacetylbenzene

By B. H. O'Connor*

Department of Physics, University of Western Australia, Nedlands, Western Australia

(*Received* 2 *April* 1973; *accepted* 29 *April* 1973)

The crystal structure of 1,3,5-triacetylbenzene has been solved and refined using 2058 intensity data collected on a Hilger & Watts diffractometer with Cu Kα radiation out to 0·632 Å^{-1} in $\sin\theta/\lambda$. The crystals are monoclinic, space group $P2_1/c$, and have unit-cell dimensions $a = 8{\cdot}386$ (3), $b = 16{\cdot}333$ (5), $c = 7{\cdot}644$ (3) Å, $\beta = 93{\cdot}69$ (3)°, with four molecules per unit cell. The positional and thermal (anisotropic for non-hydrogen atoms and isotropic for hydrogens) parameters were refined by block-diagonal least-squares calculations on $|F|^2$ with spherical-atom scattering factors. Difference maps evaluated with the X-ray data and parameters from the complementary neutron study [O'Connor & Moore (1973). *Acta Cryst.* B**29**, 1903–1909] contain features consistent with the expected bonding density. The systematic differences between the X-ray and neutron thermal parameters are due principally to the use of the spherical-atom approximation in the X-ray analysis.

Introduction

The limitations of the conventional structure-factor formalism used in analysing X-ray and neutron diffraction data have been discussed by a number of authors (*e.g.* O'Connell, Rae & Maslen, 1966; Dawson, 1967; Kurki-Suonio, 1968 and Coppens, 1969). The formalism is based on the assumption that the scattering density distribution can be adequately represented by a set of discrete spherically-symmetric scattering centres executing uncoupled harmonic vibrations. In conven-

* Present address: Department of Physics, Western Australian Institute of Technology, Bentley, Western Australia.

tional X-ray analysis any asphericity in the charge-density distribution is therefore ignored, with the result that the positional and thermal parameters are often biased. Additional parameter bias can occur in both X-ray and neutron analysis when librational and anharmonic features are not considered. It is now recognized that commercial diffractometers can provide X-ray data of sufficient accuracy for the quantitative study of asphericity in the charge density. To this end a number of analyses are being performed in this laboratory with X-ray data from organic and organometallic compounds. The organic compounds under investigation are symmetrically substituted aromatics for which the refineable parameters describing the charge density can be compared for internal consistency.

One of the principal difficulties encountered in the study of charge density is that of interaction between the positional and thermal parameters (particularly with the latter) which occurs during least-squares analysis. Clearly it is advantageous to determine the positional and thermal parameters by means of neutron diffraction. The problem of deconvoluting the charge density from X-ray data then reduces to the optimization of the atomic scattering factors. For this reason complementary X-ray and neutron analyses are being performed for some of the crystals under study.

The present paper describes the conventional X-ray structure determination (here abbreviated TABX) and qualitative charge-density study of 1,3,5-triacetylbenzene (TAB, see Fig. 1) which has been performed as an essential preliminary to the quantitative study of charge density (O'Connor & Maslen, 1973). The complementary neutron refinement (TABN) is reported in the accompanying publication (O'Connor & Moore, 1973).

Experimental

Commercial grade TAB was refined by leaching with acetone. Crystals suitable for X-ray diffraction measurements were then obtained by controlled evaporation of a solution of the refined material in acetone at ambient temperature. The crystals were colourless monoclinic prisms bounded by {100}, {010} and {001} faces. Most of the crystals had preferential development normal to the unique axis. Some, however, had comparable development of the three faces and these were therefore more suitable for intensity measurement.

The crystal selected for the diffraction measurements had dimensions 220, 250 and 320 μm for the edges [100], [010] and [001], respectively. A series of oscillation, Weissenberg and precession photographs established the space group as $P2_1/c$ and provided preliminary values for the lattice parameters. The intensity data were recorded with an automatic Hilger & Watts four-circle diffractometer (model Y230) fitted with a proportional counter and mounted on a Hilger & Watts X-ray generator (model Y50). The generator was equipped with a β-filtered Cu-target fine-focus X-ray tube. After aligning the b axis of the crystal to coincide with the φ axis of the instrument, the cell parameters were refined by a least-squares fit to ten Bragg angles measured by the Bond method.

Crystal data

$C_{12}H_{12}O_3$: 1,3,5-triacetylbenzene (TAB).
F.W. 204·23.
Space group: $P2_1/c$ (monoclinic),
$a=8{\cdot}386$ (3), $b=16{\cdot}333$ (5), $c=7{\cdot}644$ (3) Å;
$\beta=93{\cdot}69$ (3)°,
$U=1044{\cdot}8$ (7) Å^3,
$D_m=1{\cdot}27$ (by flotation), $D_x=1{\cdot}287$ g cm^{-3},
$Z=4$,
μ (calc) $=7{\cdot}75$ cm^{-1} for Cu $K\alpha$ radiation.

The intensity profiles were recorded under computer control (Jarvis, 1966) by the coupled $\theta/2\theta$-scan technique with the instrument in the 'symmetric' configuration. The scan widths for the detector were 2·4, 3·0 and 3·6°, respectively, for reflexions in the ranges of Bragg angle 0–30°, 30–60°, >60°. These widths were chosen for convenience so that the first $N/4$ and last $N/4$ points of the total N in each profile could be taken as background counts. A detector stepping increment of 0·06° was selected with a counting time of 3·31 s at each point on the profile. The total of 2058 reflexions, measured out to the limit $\sin\theta/\lambda=0{\cdot}632$ Å^{-1}, includes all accessible reflexions with the exception of the $h0l$ set (l negative) plus several reflexions which were rejected at the data reduction stage due to obvious mis-setting of the diffractometer circles. During the course of the data collection the peak intensity

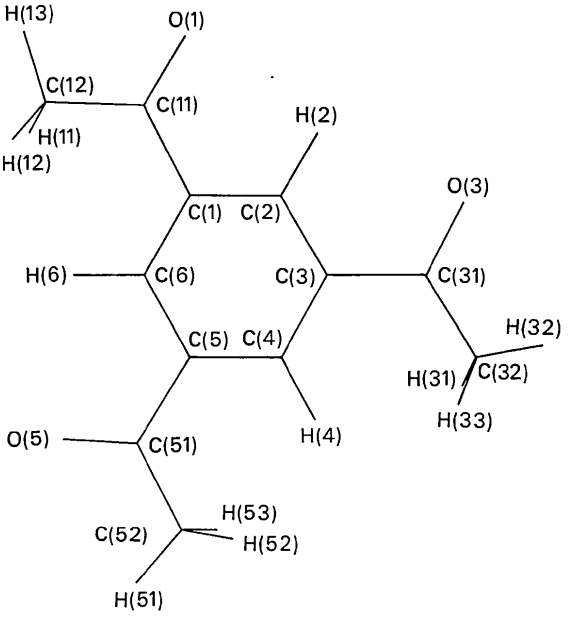

Fig. 1. Model of the molecule viewed normal to the plane of the benzene ring, with numbering system superimposed.

of the 1,14,1 reflexion was taken as a standard after every fifth profile.

In reducing the intensity profiles to estimates of integrated intensity it was assumed that the background varies linearly throughout the scan range. The intensity is then

$$I = P - B_1 - B_2$$

where P is the integrated count for the central $N/2$ points of the profile and B_1, B_2 are the background counts for the first $N/4$ and last $N/4$ points. The corresponding estimate of variance is

$$\sigma^2(I) = \sigma_1^2(I) + \sigma_2^2(I)$$

where

$$\sigma_1^2(I) = P + B_1 + B_2$$

is the variance due to counting statistics, and

$$\sigma_2^2(I) \simeq pI^2$$

is the variance due to instrumental mis-setting errors. Since the value of p had not been determined experimentally, only the $\sigma_1(I)$ could be determined at the data-reduction stage. The values of I and $\sigma_1(I)$ were corrected for Lorentz–polarization and for drift in the incident-beam intensity. Absorption errors were not applied as the maximum variation in the calculated transmission factors amounted to only $\pm 3\%$ of I for the range of data considered. The final data set of 2058 reflexions, including 1761 for which $I \geq \sigma_1(I)$, is listed in Table 1.

The *h*0*l* reflexions omitted at the data-reduction stage were measured visually from Weissenberg films and

Table 1. *Observed structure factor squares (FOSQ) and the corresponding estimated standard deviations based on counting statistics (ESD)*

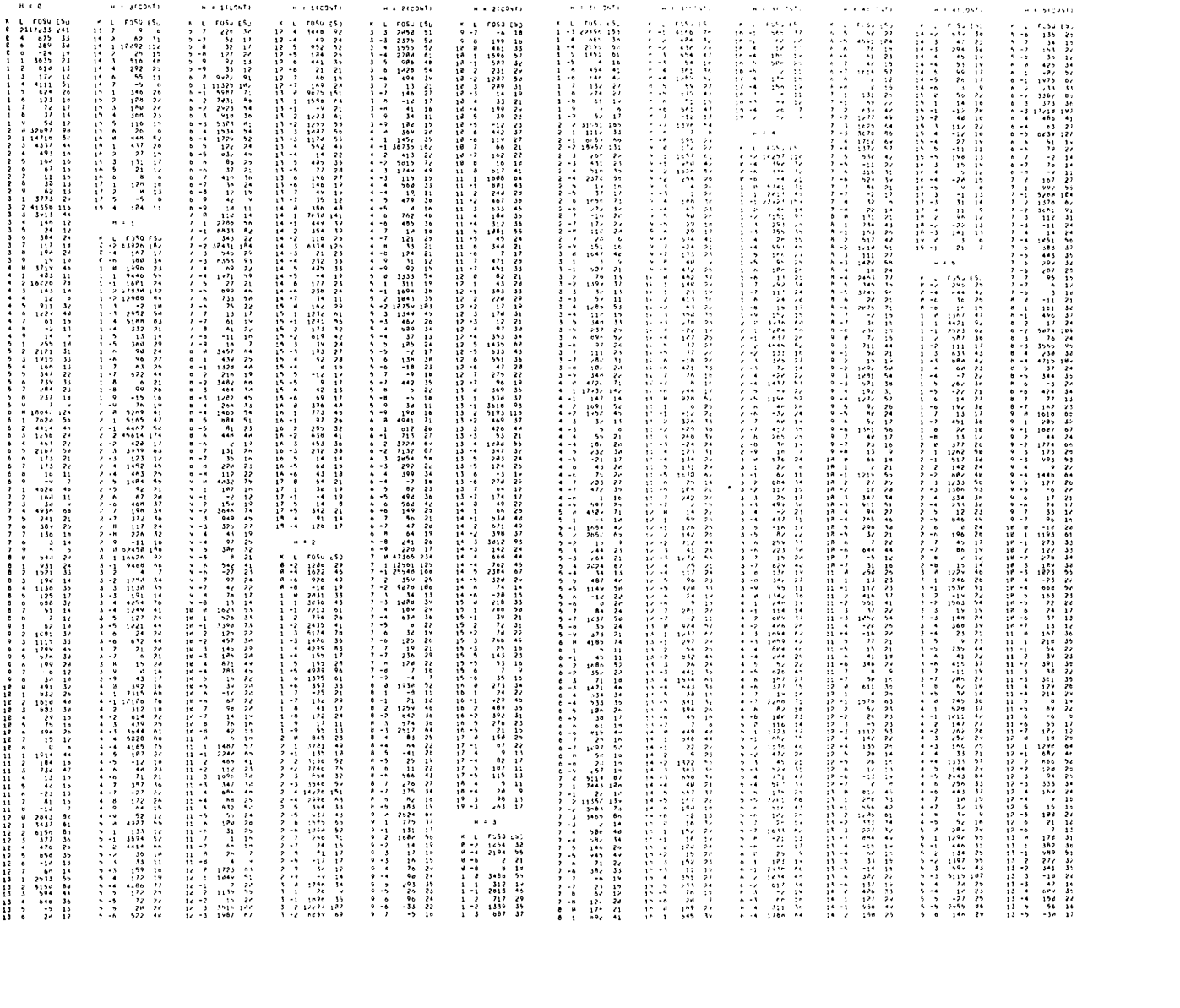

Table 1 (*cont.*)

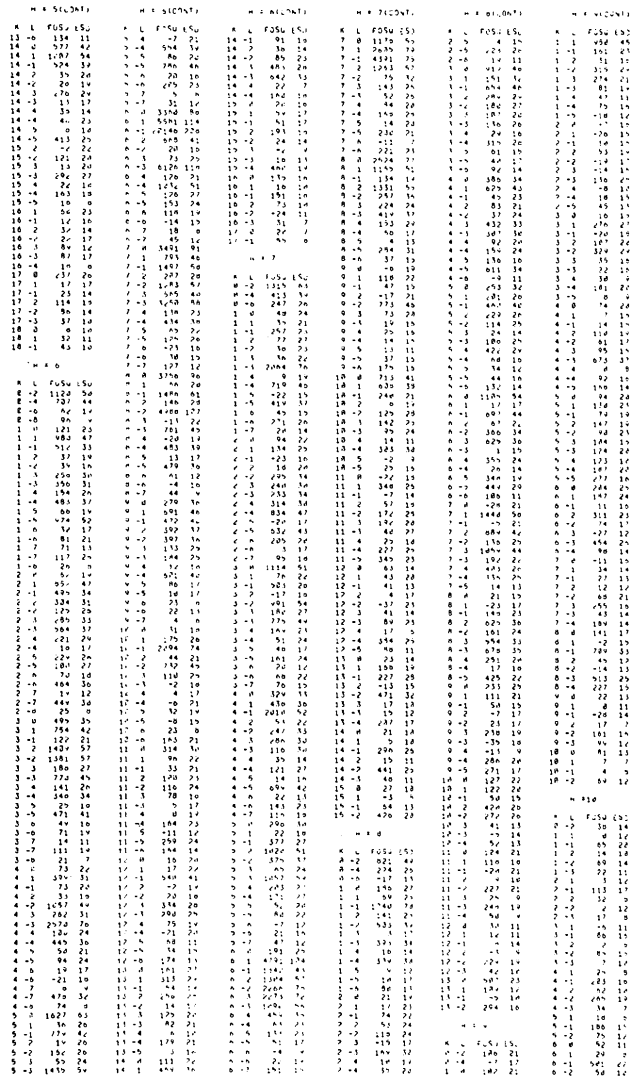

scaled to the diffractometer data in order to obtain a more complete data set for solution of the phase problem by statistical methods. The 18 photographic data thus obtained were deleted from the list of observations after the phase problem had been solved, and were not used for structure refinement.

Phase determination

The structure was solved with the aid of a series of routines written by Dr S. R. Hall of the Department of Energy, Mines and Resources (Ottawa). These routines generate the normalized structure amplitudes $|E_o(\mathbf{H})|$ which are then used to extend and refine a limited set of starting phases $\varphi(\mathbf{H})$ by repeated application of the tangent formula of Karle & Hauptman (1956). Phase generation by the tangent formula is suitable for centrosymmetric and non-centrosymmetric crystals, and therefore provides an alternative approach to the symbolic-addition procedure devised by Hauptman & Karle (1953) for centrosymmetric structures. In principle the tangent formula can be used to generate a descriptive set of $\varphi(\mathbf{H})$'s commencing with only three origin-defining phases and, in the case of non-centrosymmetric structures, an enantiomorph-defining phase.

The refinement routines cycle through successively lower $|E_o|$-thresholds since phase extension by the tangent formula is more reliable in general for reflexion triplets involving high $|E_o|$ values. The calculation examines the reliability of the estimated phases after each refinement cycle by comparing the calculated structure factors with a preset 'acceptance limit' $|E_{acc}|$, and also by testing for large oscillations in phase between successive cycles. For centrosymmetric structures, phases are also rejected if they have been determined from only one reflexion triplet.

In the present application the $|F_o|$'s were normalized to $|E_o|$'s by means of a modified Wilson-plot procedure which corrects for the effect of overall anisotropic motion (Maslen, 1967). The mean overall thermal parameters, defined such that the overall temperature factor has the form

$$\exp\left[-\bar{B}\sin^2\theta/\lambda^2-(\Delta\bar{b}_{11}h^2+\Delta\bar{b}_{12}hk+\Delta\bar{b}_{22}k^2+\Delta\bar{b}_{13}hl+\Delta\bar{b}_{23}kl+\Delta\bar{b}_{33}l^2)\right]$$

where $\bar{B}$ is the mean isotropic parameter from the conventional Wilson plot and the $\Delta\bar{b}_{ij}$ are the mean anisotropic thermal parameters, are compared in Table 2 with the values obtained by averaging the final b_{ij}'s for the non-hydrogen atoms in Table 4. Clearly the $\Delta\bar{b}_{ij}$'s correlate with the final values, and certainly in this case their introduction improved the $|E|$-distribution statistics. However, even with this improvement, the calculated statistical averages and distributions are in poor agreement with the theoretical values due principally to the degree of non-crystallographic symmetry in the molecule. The experimental values for $\langle|E|\rangle$, $\langle|E^2-1|\rangle$ and $\langle|E^2|\rangle$ are 0·716 (0·798 theoretical), 0·842 (0·968) and 0·906 (1·000), respectively, and the percentages of reflexions with $|E|>1$, $|E|>2$ and $|E|>3$ are 24·2 (32·0), 3·6 (5·0) and 0·4 (0·3), respectively.

The systematic distribution of the normalized structure factors is demonstrated in Table 3 in which are listed the fifty strongest $|E|$'s in groups according to their situation in reciprocal space, and in subgroups according to the parity of their indices. Group I contains reflexions with $h\simeq k\simeq 6$, and group II those with $h\leq 3$, $k\simeq 14$. The remainder of the reflexions constitute group III. The preferential population of the subgroups *eeo* and *oeo* within groups I and II is of general interest since this is due to the non-crystallographic symmetry of the molecule, and therefore similar problems will be experienced with any structure of this type. Note that the indices of the reflexions in groups I and II are

consistent with a specific orientation of the benzene ring. For example, the reflexions 1,14,3, $\bar{6}61$ and 761 have *d* spacings of 1·048, 1·237 and 1·075 Å, respectively, which agree reasonably well with the value 1·207 Å corresponding to half the distance between parallel C–C bonds in the benzene ring. Moreover the three interplanar angles are 110, 116 and 123°. The orientation of the molecule, although not the position, of the benzene ring in the unit cell is therefore obvious from these considerations.

The complication introduced by the systematic grouping of $|E|$'s is illustrated in the following example. If reflexions from the subgroups *eeo* (group I), *oeo* (II), and *ooo* (I) are used to specify the origin, and if the relatively few reflexions in group III are not used in phase generation, it follows that only the reflexion types *eoo* (II), *oee* (I), *ooe* (II), *eoe* (I) and *eee* (II) will be generated. Alternatively, if the origin is specified by the subgroups *eeo* (I) and *oeo* (II) which are complementary to those used in the previous specification, together with the subgroup *ooo* (I), the remaining subgroups will be generated. In effect the data in groups I and II fall into two weakly linked subsets. If tangent generation is initiated with one of these subsets, it is then inevitable that the second subset will be generated by weak indications. Therefore it is almost equally probable that the phases in the second subset will be either all correct or all incorrect.

The first attempt at phase generation using the 180 reflexions with $|E_o| \geq 1{\cdot}50$ led to a false solution. It was

Table 2. *Comparison of the mean overall anisotropic thermal parameters $\Delta\bar{b}_{ij}$ from the anisotropic scaling procedure with values from the final parameters listed in Table* 4

The Δb_{ij} are defined in the text.

	$\Delta\bar{b}_{11}$	$\Delta\bar{b}_{12}$	$\Delta\bar{b}_{22}$	$\Delta\bar{b}_{13}$	$\Delta\bar{b}_{23}$	$\Delta\bar{b}_{33}$
Anisotropic plot	−0·0018	−0·0025	−0·0005	0·0058	−0·0012	0·0027
Final parameters	−0·0001	−0·0011	−0·0005	0·0095	−0·0008	0·0101

Table 3. *The fifty strongest $|E|$'s grouped according to position in reciprocal space and subgrouped according to parity of Miller indices*

	Group I				Group II				Group III			
Subgroup	*h*	*k*	*l*	$\|E_o\|$	*h*	*k*	*l*	$\|E_o\|$	*h*	*k*	*l*	$\|E_o\|$
eeo	−6	6	1	4·23	2	14	5	3·95	−3	8	7	2·34
	−4	4	7	2·75	0	14	1	3·91				
	−6	6	3	2·59	2	14	3	2·88				
	6	6	1	2·52	2	12	5	2·54				
	−4	6	7	2·41								
	−4	6	5	2·40								
	−4	8	5	2·39								
	8	6	5	2·67								
oeo	−5	6	3	3·64	1	14	3	4·01			(nil)	
	−5	6	5	3·06	1	14	1	3·37				
	7	6	1	2·97	3	16	5	2·48				
	7	6	3	2·87	1	12	3	2·43				
	−3	4	9	2·66	3	14	5	2·33				
					3	12	7	2·29				
ooo	−7	7	1	2·57			(nil)		−3	1	3	2·46
	7	7	1	2·28								
eoo	8	7	3	2·57	2	11	7	2·48	−2	7	1	2·43
	−4	5	7	2·37					−4	1	1	2·35
oee	−5	8	4	2·45	1	12	4	2·87	1	0	2	2·75
									3	0	6	2·43
									3	2	6	2·42
									1	2	2	2·30
ooe			(nil)		1	13	0	3·18	−1	7	2	2·79
					3	13	4	2·45	1	3	0	2·44
									3	7	2	2·38
eoe			(nil)		2	13	2	2·84	2	7	0	3·26
					0	13	2	2·70				
eee	−6	8	2	2·39	0	12	2	2·58	2	2	4	2·82
									0	0	2	2·29

found somewhat difficult to select a satisfactory set of origin-defining phases since there were relatively few strong $|E_o|$'s having an odd k index, and reflexions of this type formed relatively few combinations with those reflexions having h or k odd. Eventually the trial set of linearly independent reflexions $\bar{6}61$ [*eeo* (group I)], 1,14,3 [*oeo* (II)] and $\bar{3}13$ [*ooo* (III)] were selected for origin definition. The three reflexions, which were placed at the first, second and twenty-ninth positions of the list of $|E_o|$'s, were used to generate by hand a further 25 starting phases. No contradictions were evident during the hand-generation, and subsequent comparison with values from the final structural model showed that the starting phases were all correct. The full set of 180 phases, determined by repeated application of the tangent formula with a value of 0·6 for $|E_{acc}|$, appeared reasonable according to our acceptance criteria: phase oscillations were not observed during the final cycles of the calculation, and the condition $|E_c|<1{\cdot}00$ occurred for only 8 relatively weak $|E_o|$'s.

The most obvious interpretation of the planar grid of peaks which dominated the E map (Karle, Hauptman, Karle & Wing, 1958) was that of a planar molecule superimposed on a set of redundant peaks [see Fig. 2(*a*)]. The redundant peaks were consistent with diffraction-ripple associated with the non-crystallographic symmetry elements expected in the molecule, an effect analogous to that observed when constructing structure-factor graphs for such molecules. Some of the intermolecular contacts for the proposed model were unacceptably short, and the doubt thus raised was confirmed when least-squares refinement failed to reduce the conventional R index below 0·55. Attempts to extract a model from the E map having acceptable contact distances also met with failure.

A different approach was then adopted in an attempt to obtain a satisfactory generation. The reflexions $\bar{6}61$ [*eeo* (I)], 1,13,0 [*ooe* (II)] and 102 [*oee* (III)] were selected for origin definition, and the reflexion 2,14,5 [*eeo* (II)] was assigned the symbolic phase α. Two tangent-formula generations were performed, the first with $\alpha=0$ and the second with $\alpha=\pi$. In order to reduce the probability of false generations $|E_{acc}|$ was set at 1·3 and phases were accepted only if three or more terms contributed to the tangent formula. The acceptance criteria were, therefore, more restrictive than those applied in the original generation, to the extent that the group III reflexions were removed from the calculation.

The final values of $|E_c|$ generated in the two refinement calculations were identical, and in both calculations the same 154 of the full set of 180 reflexions entered into the final calculations. Comparison of the final set of 'acceptable' phases for the two calculations showed that the reflexions for each calculation could be divided into two subsets. The phases of the reflexions within the first subset were in complete agreement for the two calculations, whereas the phases for the second subset were in complete disagreement. E maps were then constructed for the two solutions and it was found that only one, corresponding to $\alpha=0$, produced a model having sensible intermolecular contacts. The preferred E map is shown in summary form in Fig. 2(*b*).

The important point emerging from this application of the tangent-refinement procedure is that complications introduced by systematic distribution of $|E|$'s can be avoided by careful analysis of the parity sub-groups.

Structure refinement

The trial model was refined by least-squares minimization of the residual $\sum_H w[F_o^2(\mathbf{H})-F_c^2/k]^2$ with a block-diagonal approximation to the full normal equations, where k is the scale factor required to place the $F_o^2(\mathbf{H})$ set on an absolute scale and w is the estimated weight of $(F_o^2-F_c^2/k)$. The least-squares routine refines the positional and thermal parameters by segmenting the full matrix into 4×4 blocks and 9×9 blocks for iso-

Table 4. *Final fractional coordinates and anisotropic thermal parameters* ($\times10^4$) *for the non-hydrogen atoms*

The e.s.d.'s, which are enclosed in parentheses, correspond to the least significant digits in each case. The anisotropic thermal parameters are defined for a temperature factor of the form,

$$\exp[-(b_{11}h^2+b_{12}hk+b_{22}k^2+b_{13}hl+b_{23}kl+b_{33}l^2)]\,.$$

	x	y	z	b_{11}	b_{12}	b_{22}	b_{13}	b_{23}	b_{33}
C(1)	3368 (3)	3701 (2)	2899 (3)	123 (4)	8 (3)	24 (1)	52 (6)	0 (3)	175 (5)
C(2)	4893 (3)	3769 (2)	2274 (3)	126 (4)	25 (3)	27 (1)	49 (7)	0 (3)	190 (5)
C(3)	5619 (3)	4523 (2)	2132 (3)	108 (3)	16 (3)	29 (1)	29 (6)	8 (3)	142 (4)
C(4)	4810 (3)	5231 (3)	2625 (3)	106 (3)	6 (3)	26 (1)	40 (6)	5 (3)	141 (4)
C(5)	3282 (3)	5169 (2)	3237 (3)	100 (3)	12 (3)	25 (1)	41 (6)	1 (3)	144 (4)
C(6)	2575 (3)	4401 (2)	3380 (3)	107 (3)	9 (3)	27 (1)	46 (6)	3 (3)	156 (4)
C(11)	2634 (3)	2867 (2)	3028 (4)	143 (4)	12 (3)	26 (1)	120 (9)	−8 (4)	292 (7)
C(31)	7268 (3)	4558 (2)	1464 (3)	110 (3)	23 (3)	34 (1)	52 (6)	5 (3)	158 (4)
C(51)	2379 (3)	5912 (2)	3792 (3)	103 (3)	8 (3)	26 (1)	50 (6)	−21 (3)	177 (5)
C(12)	931 (4)	2784 (2)	3403 (5)	154 (5)	−19 (3)	29 (1)	157 (11)	−27 (5)	411 (10)
C(32)	8153 (3)	5350 (2)	1515 (4)	123 (4)	−8 (3)	44 (1)	138 (8)	−17 (4)	239 (6)
C(52)	2998 (3)	6748 (2)	3414 (4)	143 (4)	14 (3)	26 (1)	108 (9)	0 (4)	283 (7)
O(1)	3438 (3)	2267 (1)	2783 (5)	204 (5)	20 (3)	25 (1)	407 (13)	1 (5)	794 (13)
O(3)	7848 (2)	3942 (1)	871 (3)	153 (3)	4 (3)	39 (1)	174 (6)	−23 (3)	295 (5)
O(5)	1162 (2)	5820 (1)	4523 (3)	148 (3)	2 (3)	33 (1)	254 (7)	−40 (3)	366 (6)

tropic and anisotropic atoms, respectively, as well as a 2×2 block for $1/k$ and the 'artificial' isotropic thermal parameter. Parameter standard deviations are estimated in the usual manner as

$$\sigma_i = G(a^{ii})^{1/2}$$

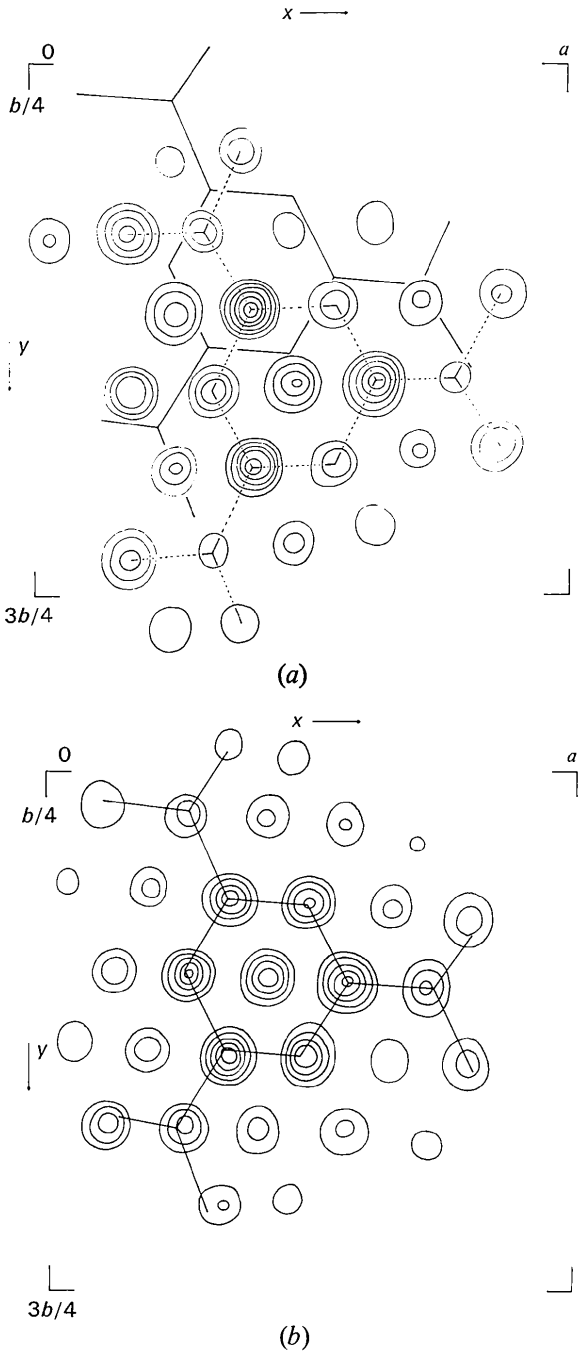

Fig. 2. *E*-maps viewed down **c*** for (*a*) the incorrect phase set and (*b*) the correct phase set. The model selected for the incorrect set is indicated by broken lines; the correct model by unbroken lines. Contours at arbitrary but equal intervals.

where a^{ii} is the diagonal element for parameter i of the inverse to the appropriate block matrix, and G is the 'goodness-of-fit' index defined as

$$G=[\sum w(F_o^2-F_c^2/k)^2/(m-n)]^{1/2}$$

for m total observations and n refinable parameters.

All reflexions were included at the measured value of F_o^2, including those with small negative values, rather than setting some arbitrary 'limit of observation' since that concept is meaningless for diffractometer data and serves only to reduce the R index at the expense of precision in the parameters (O'Connor & Valentine, 1969). Standard X-ray scattering factors for spherically-symmetric atoms were used in all calculations: the neutral atom scattering factors based on SCF wave functions with exchange (*International Tables for X-ray Crystallography*, 1968) for carbon and oxygen, and the hydrogen scattering factor tabulated by Stewart, Davidson & Simpson (1965). The twelve hydrogen atoms were located without ambiguity from a difference synthesis.

The final least-squares calculations were performed with estimated absolute experimental weighting factors. The proportionality constant p in the expression for $\sigma_2^2(I)$ was determined from an analysis of structure-factor agreement with the approximation

$$p\simeq\sum\pi/2(F_o^2-F_c^2)^2/\sum(F_o^2)^2-\sum\sigma_1^2(F_o^2)/\sum(F_o^2)^2.$$

This procedure gave a value of 0·0090 for p. Four refinement cycles with absolute weights reduced all parameter shifts to insignificant values. The index G (which is ideally *one* for a model completely refined with experimental weights) was thereby reduced from 1·520 to a final value of 1·329, and the R indices $R(F^2)$* and $R(F)$ to final values of 0·104 and 0·093. The corresponding R indices for the 3σ data [*viz.* the set with $F_o^2\geq3\sigma_1(F_o^2)$] were 0·099 and 0·076.

The final parameters for the non-hydrogen and hydrogen atoms are presented in Tables 4 and 5, respectively.

* $R(F^2)=\sum|F_o^2-F_c^2|/\sum F_o^2$, $R(F)=\sum|F_o-F_c|/\sum F_o$.

Table 5. *Final fractional coordinates* ($\times10^3$) *and isotropic thermal parameters* (Å$^2\times10$) *for the hydrogen atoms*

The e.s.d.'s, enclosed in parentheses, are quoted for the least significant digits in each case. The isotropic thermal parameters, B, are Debye–Waller factors.

	x	y	z	B
H(2)	533 (3)	330 (2)	193 (4)	53 (7)
H(4)	530 (3)	574 (2)	258 (3)	39 (6)
H(6)	158 (3)	436 (2)	370 (3)	45 (6)
H(11)	36 (5)	308 (3)	241 (5)	107 (12)
H(12)	88 (5)	303 (3)	459(5)	98 (11)
H(13)	39 (7)	221 (3)	314 (6)	119 (13)
H(31)	824 (4)	551 (2)	262 (4)	54 (7)
H(32)	914 (5)	527 (2)	115 (5)	88 (10)
H(33)	764 (3)	583 (2)	89 (4)	51 (7)
H(51)	234 (5)	712 (2)	379 (5)	97 (11)
H(52)	410 (4)	679 (2)	399 (4)	69 (8)
H(53)	314 (4)	683 (2)	208 (4)	79 (9)

Discussion

In view of the influence of asphericity on the positional and thermal parameters obtained in the TABX work, the molecular geometry and thermal motion are discussed in the TABN paper rather than here. The major point of interest emerging from the present analysis is the degree of asphericity evident in Fourier syntheses, plus the extent of systematic error in the final TABX parameters.

Charge distribution

In principle, the form of the valence charge distribution can be represented by Fourier difference syntheses involving the observed X-ray structure factors and the calculated spherical-atom structure factors, as discussed in detail by Coppens (1967). Two types of syntheses, designated $\Delta\varrho(X)$ and $\Delta\varrho(N)$, are of interest. The $\Delta\varrho(X)$ synthesis is based on positional and thermal parameters from the conventional X-ray least-squares refinement, while the $\Delta\varrho(N)$ synthesis is computed with conventional neutron parameters. Both types of map should contain similar bonding features with those in $\Delta\varrho(X)$ generally less prominent. Owing to the distribution of valence electrons, each atom site in the difference map should reside within a region of negative density, and for the non-hydrogen atoms there should be an antisymmetric distribution about each atomic site.

The $\Delta\varrho(X)$ map within the best plane for the central twelve atoms is shown in Fig. 3(*a*). The distribution of peaks is essentially antisymmetric, although some of the expected peaks are barely above background. While least-squares refinement appears to have eliminated much of the bonding density, it is obvious that the parameters in the conventional X-ray refinement cannot entirely absorb bonding features.

The $\Delta\varrho(N)$ synthesis for the molecular plane is summarized in Fig. 3(*b*). The features are more intense than those in $\Delta\varrho(X)$, and are entirely consistent with elementary valence-bond concepts. There are pronounced peaks close to most bond centres, corresponding to σ-bond overlap density. It should be noted that the oxygen and methyl carbon atoms deviate from the central plane of the molecule by 0·16 and 0·21 Å, respectively, owing to rotation of the acetyl groups about the C(sp^2)–C(sp^2) bonds. Accordingly the features in the vicinity of each acetyl group in the difference maps vary somewhat from those within the exact plane of each group. The three-dimensional map gives a clearer indication of the oxygen lone-pair electron distributions. Note also that the relatively high degree of thermal motion associated with the acetyl groups results in some loss of definition in the bonding features within the groups.

Sections of the $\Delta\varrho(N)$ map in the bond planes normal to the plane of the molecule are shown in Fig. 4(*a*) and (*b*). The bonding density peaks and the hollows at the atomic sites are elongated in the direction of the normal to the molecular plane, an effect also observed by Coppens, Sabine, Delaplane & Ibers (1969) in a similar analysis of oxalic acid dihydrate. Elonga-

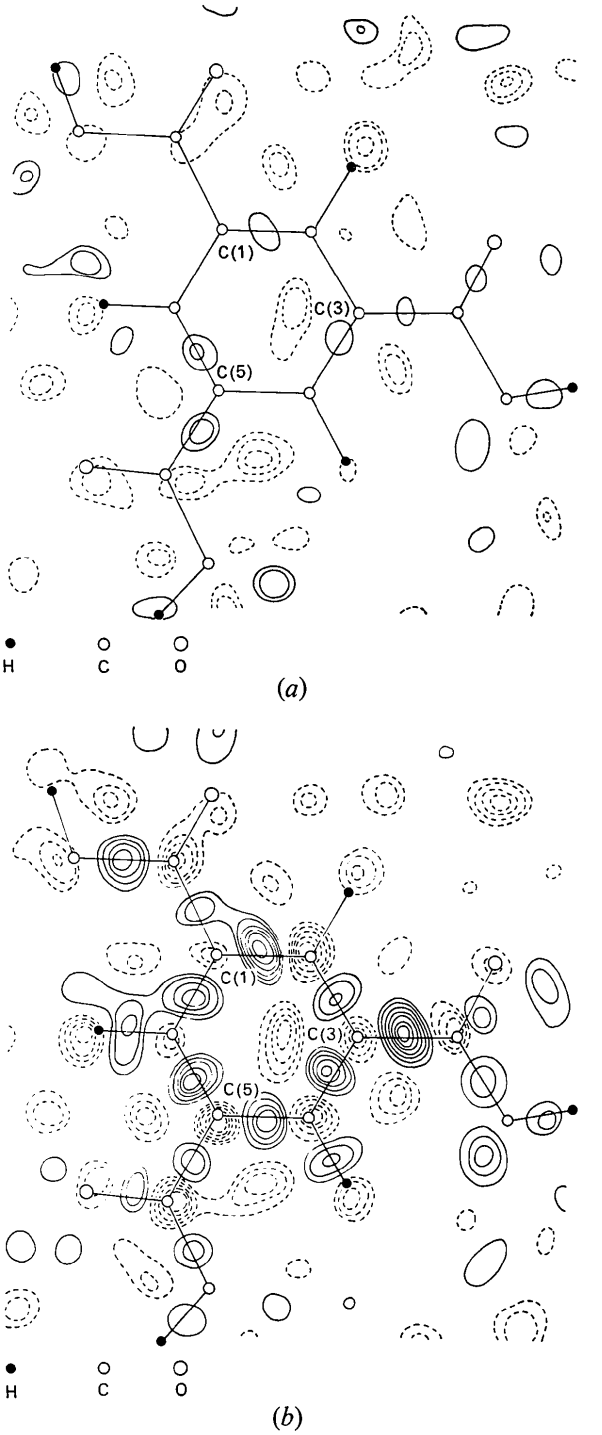

Fig. 3. Difference maps through the best plane of the molecule. (*a*) $\Delta\varrho(X)$ map generated with X-ray parameters. (*b*) $\Delta\varrho(N)$ map generated with neutron parameters. Positive and negative contours are shown as unbroken and broken lines, respectively. First contour at 0·10 e Å^{-3}. Contour interval: 0·05 e Å^{-3}.

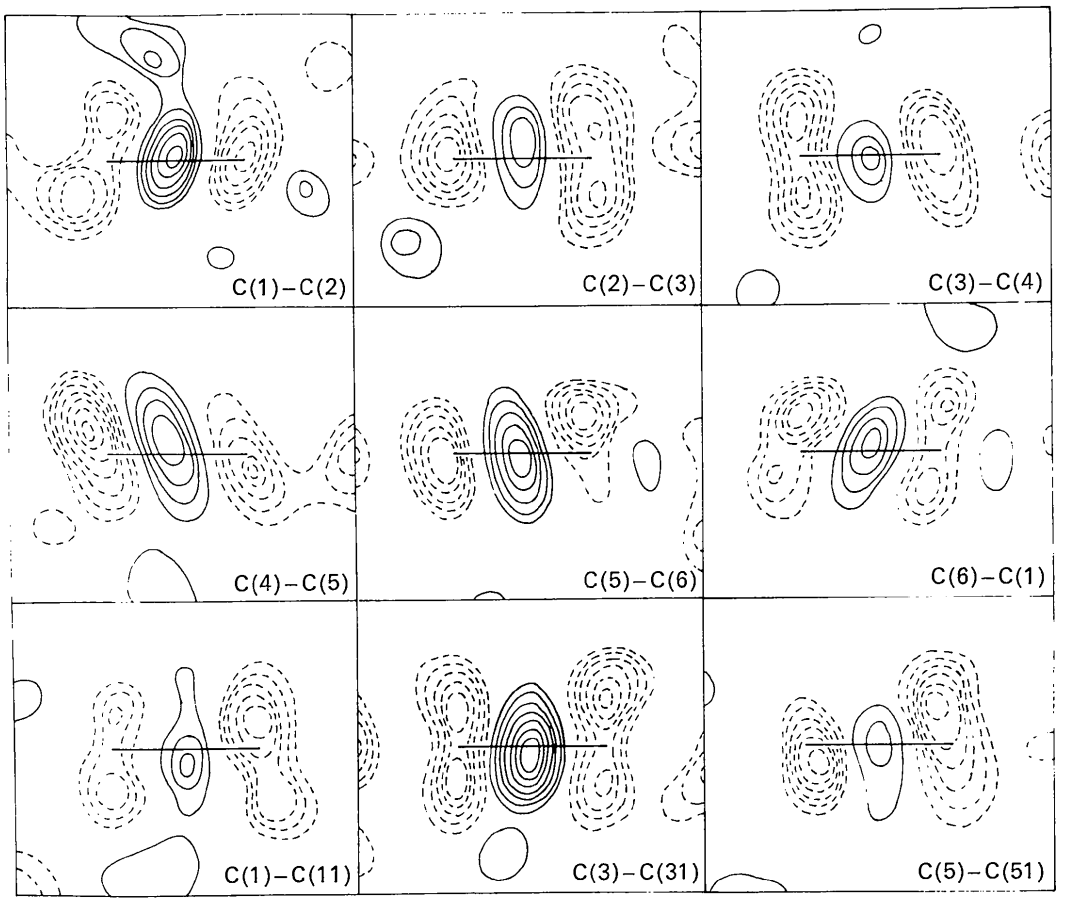

(*a*)

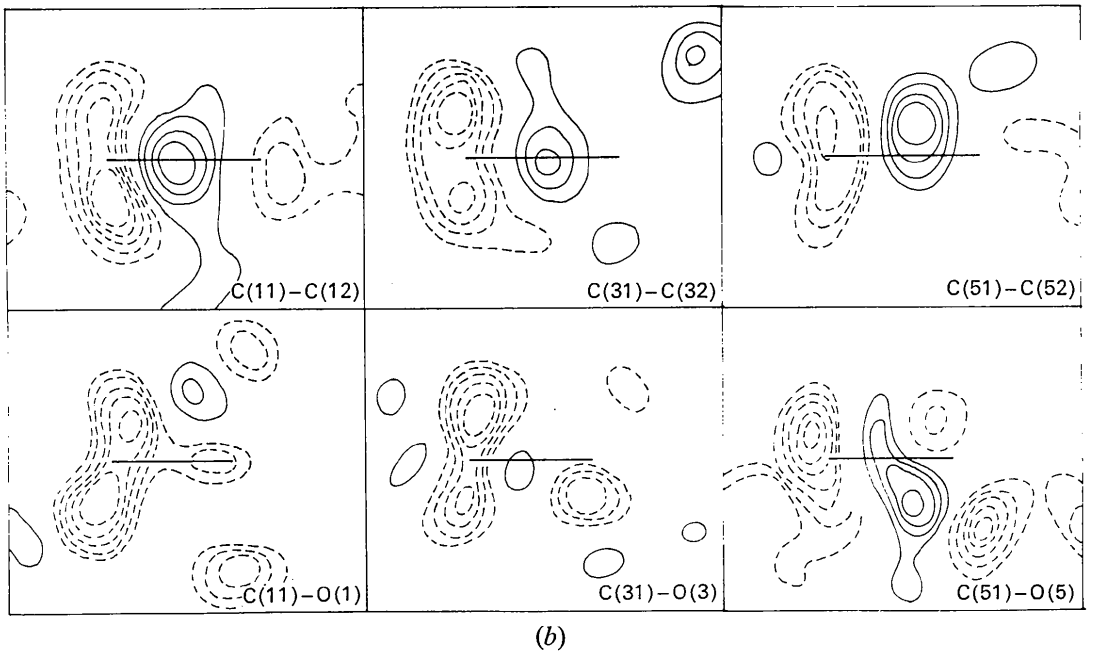

(*b*)

Fig. 4. Difference maps through the bonds (*a*) normal to the plane of the ring, (*b*) normal to the plane of the appropriate acetyl group. Conventions and contour data as for Fig. 3.

tion of a bond peak can be attributed to the influence of π-character in the bond. In TAB the effect is most pronounced for the C–C(ring) and C(sp^2)–Csp^2) bonds, and minimal for the C(sp^2)–C(sp^3) bonds. On theoretical grounds, there should be appreciable π-character associated with the C–C(ring) bonds and none with the C(sp^2)–C(sp^3) bonds. The observations are therefore consistent with theory, although the conclusion that there is π-character associated with the C(sp^2)–C(sp^2) bonds is less predictable as it indicates conjugation between the ring and acetyl groups. This point is considered further in the TABN paper. It is disappointing that the bonding features in the vicinity of the C–O bonds are not clearly defined, owing probably to the excessive thermal motion of the oxygen atoms.

In general the TAB maps are similar in definition to those reported for *sym*-triazine (Coppens, 1967), oxalic acid dihydrate (Coppens *et al.*, 1969), and cyanuric acid (Coppens & Vos, 1971). The results of all four investigations demonstrate the value of using the $\Delta\varrho(N)$ synthesis to display the electron-density distribution. The consistency of this synthesis with basic valence-bond concepts highlights its application in bonding studies at the qualitative level. Further, if it is intended to conduct a quantitative analysis of electron density using reciprocal-space procedures, inspection of the $\Delta\varrho(N)$ synthesis is a most useful preliminary as it gives a clear indication of the significance of bonding effects in the experimental data.

Systematic error in the positional and thermal parameters

It has been found in similar studies that asphericity shifts in the X-ray positions of non-hydrogen atoms have an upper limit of approximately 0·01 Å. For TAB the differences range from 0·005 (7) Å for C(3) to 0·013 (8) Å for C(32), but these are not of sufficient accuracy to be considered significant.

The hydrogen X-ray positions show the usual bias with the smallest difference being 0·05 (7) Å for H(53) and the largest difference 0·30 (7) Å for H(13). These effects result in contraction of the C–H distances in TABX, the average values being 0·93 and 0·97 Å for the C–H(ring) and C–H(acetyl) bonds, respectively, compared with the corresponding values of 1·08 and 1·04 Å obtained in the neutron study.

The differences between the U_{ij} vibration components of the non-hydrogen atoms, obtained in the TABX and TABN refinements, are listed in Table 6. The U_{ij} tensors are defined relative to the molecular axial system with axis 1 along the vector C(6)–C(3), axis 2 along C(1)–C(5), and axis 3 normal to the plane of the molecule. The X-ray vibration amplitudes within the plane of the molecule exceed the neutron values, and the opposite effect is observed along the normal to the plane. Assuming that the neutron values are relatively free of systematic error, it can be concluded that the observed differences are consistent with a concentration of bonding density in the plane being absorbed to a large extent by the X-ray thermal parameters.

The author is grateful to Dr E. N. Maslen for his constant interest in the study, and to the Australian Research Grants Committee for financial support. During the course of the work the author was in receipt of a Queen Elizabeth Fellowship.

References

COPPENS, P. (1967). *Science*, **158**, 1577–1579.
COPPENS, P. (1969). *Acta Cryst.* A**25**, 180–186.
COPPENS, P., SABINE, T. M., DELAPLANE, R. G. & IBERS, J. A. (1969). *Acta Cryst.* B**25**, 2451–2458.
COPPENS, P. & VOS, A. (1971). *Acta Cryst.* B**27**, 146–158.
DAWSON, B. (1967). *Proc. Roy. Soc.* A**298**, 264–288.
HAUPTMAN, H. & KARLE, J. (1953). *Solution of the Phase Problem. I. The Centrosymmetric Crystal.* A.C.A. Monograph No. 3. Pittsburgh Polycrystal Book Service.
International Tables for X-ray Crystallography (1968). Vol. III, 2nd ed., pp. 202–203. Birmingham: Kynoch Press.

Table 6. *Vibration components* ($Å^2 \times 10^4$) *for the non-hydrogen atoms referred to the molecular axial system*

Symbol X denotes parameters from the X-ray refinement, and X–N the difference between the corresponding parameters from the X-ray and neutron refinements.

	U_{11}		U_{12}		U_{22}		U_{13}		U_{23}		U_{33}	
	X	X–N	X	X–N	X	X–N	X	X–N	X	X–N	X	X–N
C(1)	409	49	21	−13	331	33	10	42	28	−16	534	−76
C(2)	438	68	78	17	361	21	−12	21	42	−27	568	−31
C(3)	378	91	43	−8	389	42	2	11	44	−1	420	−87
C(4)	355	38	14	−14	361	21	16	49	28	14	430	−7
C(5)	340	51	38	14	336	29	4	24	25	1	436	−28
C(6)	359	15	28	7	370	58	5	41	29	−5	474	−69
C(11)	449	50	41	25	346	31	−17	34	44	−38	903	−54
C(31)	370	71	77	−13	460	33	11	−2	44	−8	484	−91
C(51)	356	48	51	13	340	28	−24	11	−23	−28	542	−60
C(12)	485	53	−44	−12	385	−22	−89	−2	−14	−2	1255	4
C(32)	333	−11	16	15	578	44	37	32	−43	−49	795	−1
C(52)	459	−8	38	24	351	33	−19	60	65	9	863	−46
O(1)	529	3	38	20	357	13	−153	74	227	−17	2445	−78
O(2)	429	7	156	6	506	−6	43	0	15	8	973	−24
O(3)	338	16	69	17	418	−3	56	51	−43	−10	1243	−124

JARVIS, R. A. (1966). *J. Sci. Instrum.* **43**, 899–907.
KARLE, J. & HAUPTMAN, H. (1956). *Acta Cryst.* **9**, 635–651.
KARLE, I. L., HAUPTMAN, H., KARLE, J. & WING, A. B. (1958). *Acta Cryst.* **11**, 257–263.
KURKI-SUONIO, K. (1968). *Acta Cryst.* A**24**, 379–390.
MASLEN, E. N. (1967). *Acta Cryst.* **22**, 945–946.
O'CONNELL, A. M., RAE, A. I. M. & MASLEN, E. N. (1966). *Acta Cryst.* **21**, 208–219.
O'CONNOR, B. H. & MASLEN, E. N. (1973). *Acta Cryst.* To be published.
O'CONNOR, B. H. & MOORE, F. H. (1973). *Acta Cryst.* B**29**, 1903–1909.
O'CONNOR, B. H. & VALENTINE, T. M. (1969). *Acta Cryst.* B**25**, 2140–2144.
STEWART, R. F., DAVIDSON, E. R. & SIMPSON, W. T. (1965). *J. Chem. Phys.* **42**, 3175–3187.

Acta Cryst. (1973). B**29**, 1903

Neutron-Diffraction Refinement of the Crystal Structure of 1,3,5-Triacetylbenzene

BY B. H. O'CONNOR*
Department of Physics, University of Western Australia, Nedlands, Western Australia

AND F. H. MOORE
Australian Institute of Nuclear Science and Engineering, Lucas Heights, New South Wales, Australia

(*Received* 2 *April* 1973; *accepted* 29 *April* 1973)

A neutron-diffraction investigation of the crystal structure of 1,3,5-triacetylbenzene has been performed in parallel with an X-ray diffraction analysis, as part of a study of electron-density distribution. Data were collected with two crystals at a neutron wavelength of 1·192 Å, the total number of 1576 independent reflexions being limited to a maximum of 0·57 $Å^{-1}$ in $\sin\theta/\lambda$. The positional and anisotropic thermal parameters were refined by block-diagonal least-squares calculations on $|F|^2$ with allowance for extinction effects in the data. The final model is discussed with reference to the intra- and intermolecular geometry and thermal motion.

Introduction

The present investigation (here abbreviated TABN) of the crystal structure of 1,3,5-triacetylbenzene (TAB) has been performed to complement the X-ray study (TABX) of TAB described in the accompanying paper by O'Connor (1973). Combined X-ray and neutron diffraction studies of organic molecules have been used, for example, by Coppens (1967), Coppens, Sabine, Delaplane & Ibers (1969) and Coppens & Vos (1971) to investigate the nature of the charge-density distribution in, respectively, *sym*-triazine, oxalic acid dihydrate and cyanuric acid. The advantage of using combined analyses for this purpose is that positional and thermal parameters obtained with neutron parameters can thus be employed with the X-ray data to construct Fourier difference maps which ideally reflect only the inadequacies of the spherical atom approximation (see TABX). If the expected bonding features are evident in the difference maps, it is then most useful to attempt a least-squares study of the valence-electron distribution, in which the positional and thermal parameters are fixed at the neutron values.

The details of molecular geometry and thermal motion are discussed in this paper rather than in the TABX account because of the general superiority of the neutron parameters.

Experimental

The sample of TAB which had been used to grow crystals for the TABX study was purified further by successive recrystallizations from acetone. It was then a simple matter to obtain crystals of sufficient volume for neutron diffraction by seeding a saturated solution of TAB in acetone. The crystals were all monoclinic prismatic with development of the {100}, {010} and {001} faces and were characterized by preferential growth normal to the unique axis. The intensity data were recorded with two crystals, the dimensions of which are given in Table 1. The smaller specimen (crystal 1) was used to measure the low-angle reflexions

Table 1. *Crystal dimensions*

Face indices	D^*(Crystal 1)	D^*(Crystal 2)
$\left.\begin{matrix}1\,0\,0\\ \bar{1}\,0\,0\end{matrix}\right\}$	0·040 cm	0·120 cm
$\left.\begin{matrix}0\,1\,0\\ 0\,\bar{1}\,0\end{matrix}\right\}$	0·224	0·480
$\left.\begin{matrix}0\,0\,1\\ 0\,0\,\bar{1}\end{matrix}\right\}$	0·470	0·762

* Length of normal between the specified pair of faces.

* Present address: Department of Physics, Western Australian Institute of Technology, South Bentley, Western Australia.